Guest-Tuned Spin Crossover in Flexible Supramolecular Assemblies Templated by a Halide (Cl^-, Br^- or I^-).

M. D. Darawsheh,[a] L. A. Barrios[a], O. Roubeau[b], S. J. Teat[c] and G. Aromí*[a]

Ligand 1,3-bis(3-(pyridin-2-yl)-1H-pyrazol-5-yl)benzene, L, forms mononuclear spin crossover complexes $[FeL_3]^{3+}$ with pendant arms that cause them to dimerize through numerous intermolecular interactions forming supramolecular $[X@[FeL_3]_2]^{3+}$ cations. These have the flexibility to encapsulate Cl^-, Br^- or I^-, which allow tunning the magnetic properties, in the solid state and in solution.

Supramolecular chemistry relies on weak chemical interactions to see the formation of architectures beyond the molecule, following a process of molecular recognition between otherwise, stable components.[1, 2] The range of intermolecular interactions encompass hydrogen bonds, π···π, C–H···π, cation···π or anion···π interactions,[3] and, because of their often encountered lability, also coordination bonds.[4, 5] This field provides invaluable tools for the design and preparation of molecular machines and functional devices.[6-8] Thus, molecular recognition may induce the assembly of individual components with interesting properties, such as magnetic,[9] optical[10] or electronic,[11] in useful forms. In this context, supramolecular chemistry has been exploited for the construction of intricate assemblies exhibiting spin crossover (SCO) properties.[12-20] However, only in very rare cases such assemblies constitute cages also capable of recognizing and encapsulating guests *via* non-covalent forces, thereby influencing the SCO process.[12, 21, 22] We recently prepared and exploited the capacity of the bis-chelating ligand 1,3-bis(3-(pyridin-2-yl)-1H-pyrazol-5-yl)benzene, L (Scheme 1) for the synthesis of dinuclear Fe(II) triple stranded helicates that form upon encapsulation of a Cl^- or a Br^- ion.[23] The latter is stabilized within the cavity of the helicate through hydrogen bonds involving the N–H groups of L. Interestingly, the specific nature of the guest exerts a sizeable influence on the temperature of the SCO of the supramolecular assembly. However, the limited flexibility of the dinuclear ensemble allows only the confinement of Cl^- or Br^- while a guest of the size of I^- cannot be hosted. We report here a markedly different supramolecular arrangement of the Fe(II)/L/X^- system, $(X@[FeL_3]_2)^{3+}$, with the flexibility to admit the formation of the series with Cl^-, Br^- and I^-. The assembly consists of a dimer of two mononuclear $[FeL_3]^{2+}$ moieties that are firmly held together following the inter-digitation of the uncoordinated arms of the ligands L, and through the template effect of the encapsulated anion X^-. Its nature directly affects the SCO process of the Fe(II) ions.

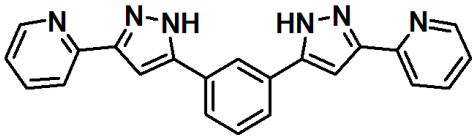

Scheme I. Molecular structure of ligand L.

The aerobic reaction in methanol of L and FeX_2 (X=Cl, Br) using the 3:2 molar ratio of L *vs*. Fe, produces over time, in contact with an aqueous solution of NH_4PF_6, crystals of the supramolecular double salt $(X@[FeL_3]_2)(OH)(PF_6)_2$ (**1**, Cl; **2**, Br). This reactivity is in striking contrast to that producing the previously described dimetallic helicate-cations $(X@[Fe_2L_3])^{3+}$.[23] A possible explanation is that the aqueous media favours now the partial oxidation of Fe(II), modifying the stoichiometry while also increasing the basicity of the medium. Another difference with the dimetallic $(X@[Fe_2L_3])^{3+}$ host-guest system is that the new arrangement is more flexible, thus allowing the incorporation of the larger guest iodide. The reaction with FeI_2, L and NH_4PF_6 did not produce any crystals. However, when conducted in pure methanol, it yields the analogous supramolecular dimer of monomers $(I@[FeL_3]_2)^{3+}$ (cation of **3**, characterized in a lattice with the anions PF_6^-, I^- and I_3^- in fractional amounts; see SI). This composite cation is also obtained from a reaction in methanol between $Fe(CF_3SO_3)_2$, L (1:3 ratio of Fe *vs*. L) and excess of NBu_4I, which produces the complex salt $(I@[FeL_3]_2)I_2(I_3)_{0.6}(OH)_{0.4}$ (**4**). Interestingly, excess of $FeCl_2$ does not facilitate the formation of the iron-rich helicate; equimolar amounts of $FeCl_2$ and L, now with acetone as solvent, again result into the dimer of Fe(II) complexes templated by a central Cl^- ion. The crystallization takes place upon layering with toluene, revealing the presence of iron(III) tetrachloride anions, namely $(Cl@[FeL_3]_2)(FeCl_4)_3$ (**5**). These anions result from partial aerial oxidation of Fe(II), not uncommon in such kind of reactions.[18] The above five compounds are obtained as red crystals in low yield (3-13%).

The molecular structure of compounds **1** to **5** was determined by single crystal X-ray diffraction (Table S1). Their main feature is the supramolecular assembly $(X@[FeL_3]_2)^{3+}$ (X^-=Cl^-, Br^-, I^-). It is formed by two entangled mononuclear $[FeL_3]^{2+}$ cations (Figs. 1 and S1), each consisting of one Fe(II) center, bound to three pyrazolylpyridine didentate moieties of three ligands L, furnishing the metal with a distorted octahedral environment. For all compounds, the Fe–N distances at 100 K correspond to the low spin (LS) state for Fe(II) (average of 1.950 for **1**, Table S2 for the rest). The second chelating arm of L is not coordinated. Instead, the three ligands are engaged in an extensive array of intermolecular interactions with their counterparts from the other $[FeL_3]^{2+}$ component, yielding a helical supramolecular arrangement that encapsulates a Cl^- (**1** and **5**), a Br^- (**2**) or an I^- (**3** and **4**) guest. These anions exhibit a total of six N–H···X^- hydrogen bonds, one with each of the six L ligands of the $(X@[FeL_3]_2)^{3+}$ dimer of monomers. In addition, each ligand L is poised for an additional strong hydrogen bond of the type N–H···N with an equivalent ligand from the opposite $[FeL_3]^{2+}$ species of the assembly (Figs. 2, S2, Table S3).

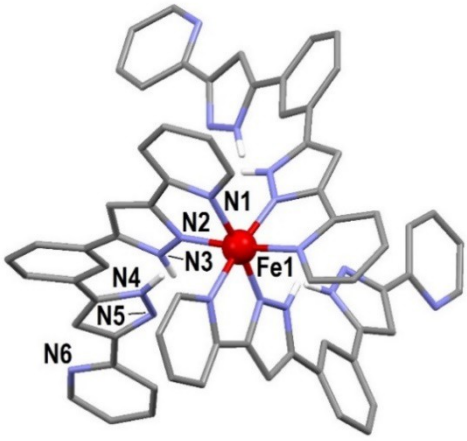

Figure 1. Representation of the mononuclear $[FeL_3]^{2+}$ complex cation composing the supramolecular assembly of **1**. Unique heteroatoms are labelled and C atoms are grey. Only H atoms of N–H groups are shown (white). The same moiety is present in **2** to **5**.

In addition to twelve hydrogen bonds, the supramolecular assembly is cemented by an extensive series of π···π interactions; each ligand is disposed in front of its counterpart from the other $[FeL_3]^{2+}$ unit, engaging in five aromatic contacts (Fig. 3). Therefore, an impressive total of fifteen π-stacking interactions contribute to the stability of the $(X@[FeL_3]_2)^{3+}$ host-guest assembly of monometallic complexes. Indeed, the cumulative effect of van der Waals interactions possibly competes with the formation of additional Fe–N coordination bonds that would lead to the dinuclear $(X@[Fe_2L_3])^{3+}$ assembly. The volume of the cavity enclosing the X^- anion increases with the size of the latter (Table 1), ranging from 30 (**1**), to 35 (**2**) to 48 Å^3 (**3**), as measured using Swiss-Pdb Viewer 4.1 (Fig. S3).[24] This underscores the flexibility of the assembly adapting to the size of the guest, as reflected by a progressive elongation of the N–H···X^- and N–H···N hydrogen bonding distances (Table 1) while the Fe···Fe and Fe···X separations remain similar (Tables 1, S2, S3).

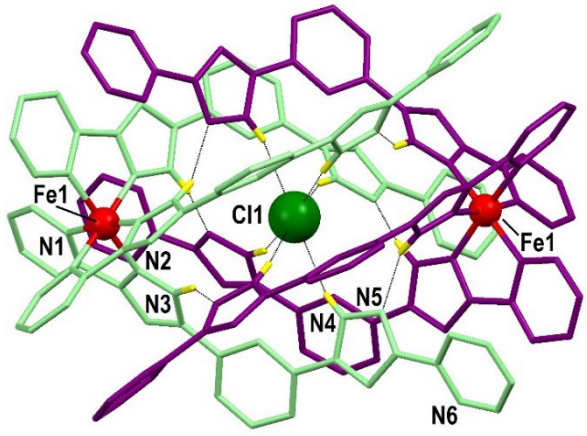

Figure 2. Representation of the $(X@[FeL_3]_2)^{3+}$ supramolecular assembly in **1** (X=Cl^-). The ligands of each $[FeL_3]^{2+}$ unit are in a different colour (green and purple, respectively). Unique heteroatoms are labelled. Only H atoms of N–H groups are shown (yellow). The same moiety is present in **2** to **5**.

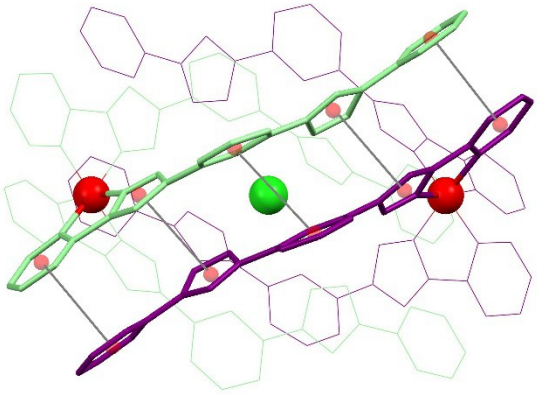

Figure 3. Representation of the $(X@[FeL_3]_2)^{3+}$ supramolecular assembly in **1** to **5**, emphasizing one of the three sets of interactions between pairs of L ligands from different $[FeL_3]^{2+}$ components. In this highlighted pair of ligands, centroids of interacting rings are linked by a grey line. The ligands of each $[FeL_3]^{3+}$ unit are in a different colour (green and purple, respectively).

Table 1. Structural parameters relevant to the encapsulation of X^- (X^- = Cl^-, Br^-, I^-) within the $(X@[FeL_3]_2)^{3+}$ assembly in **1** to **5**.

X^-	[a]N–H···X^-	[a]N–H···H	[b]$r(X^-)$	Fe···Fe	[c]V_{CAVITY}
Cl^- (**1**)	3.38(1)	2.78(2)	163.5	11.475	30
Br^- (**2**)	3.453(2)	2.812(4)	178.8	11.388	35
I^- (**3**)	3.50(5)	2.85(7)	201.5	11.498	48
I^- (**4**)	3.48(2)	2.86(3)	201.5	11.464	-
Cl^- (**5**)	3.39(3)	2.82(4)	163.5	11.706	-

[a]Average values (Å). [b]Values in pm.[25] [c]Internal cavity of the host for encapsulation of the X^- guest as measured using Swiss-Pdb Viewer 4.1.[24]

In addition to the intra-dimer hydrogen bonds, the dimer of monomers $(X@[FeL_3]_2)^{3+}$ of compounds **1** to **5** establish such interactions with external components of the lattice via the distal, not coordinated pyridyl groups of the ligands, which are all rotated towards the exterior of the helical assembly. In **1**, **2** and **4**, the interactions are with either OH^- or H_2O moieties, which share the same crystallographic location by virtue of occupational disorder Fig. S4). In **3**, these are with MeOH molecules or weak C–H···N contacts involving neighbouring complexes. For complex **5**, only C–H···N interactions are occasionally encountered. The crystal lattice of **1**, **2** and **4** consists of rods of $(X@[FeL_3]_2)^{3+}$ units parallel to the Fe···Fe axis connected through their ends *via* six complementary C–H···π interactions involving the coordinated pyridyl rings (Fig. S5). These rods interact through the hydrogen bonds with OH^- or H_2O species or *via* lateral C–H···π interactions (Fig. S6), while leaving space in between them for the accommodation of PF_6^- anions. In compound **3**, the $(I@[FeL_3]_2)^{3+}$ assemblies of monomers are organized in sheets that alternate with hydrophilic layers composed by the anions (PF_6^-, I^- and I_3^-; Fig. S7). Within layers, the helicates interact through π···π and C–H···π interactions. The $(Cl@[FeL_3]_2)^{3+}$ moieties of **5** are connected pairwise by six C–H···π interactions, and these dimers interact to each other through their aromatic rings.

The coordination environment of Fe(II) in compounds **1** to **5** is suitable to produce SCO phenomena.[21, 23, 26] The only difference among these compounds susceptible to influence their magnetic properties is the nature of the guest X^- within the $(X@[FeL_3]_2)^{3+}$ assembly. As representative examples, the bulk magnetic susceptibility

of compounds **1** (Cl^-), **2** (Br^-) and **4** (I^-) was determined in the 5-395 K temperature range under a constant magnetic field of 0.5 T. The results are represented in Fig. 4 as $\chi_M T$ *vs* *T* plots (where χ_M is the molar paramagnetic susceptibility). Below near 250 K, the value of $\chi_M T$ is nearly constant for all compounds and within the 0.1 to 0.3 cm^3Kmol^{-1} range. This means that in this temperature range, 95% or more of the Fe(II) centers lay in the low spin (LS) state for the three compounds. Immediately above this temperature, the $\chi_M T$ product for **4** raises suddenly, indicating the occurrence of SCO, reaching a 60% of completion. A similar behaviour was observed at much higher temperatures (near 350 K) for the Cl and Br analogues (**1** and **2**), with approximate conversions of 30 and 60%, respectively, at 395 K. The somewhat irregular shape of the curves may be caused by simultaneous processes of solvent desorption, affecting the molar mass of the compounds and known to influence the SCO behaviour. [23, 27] This hampers a clear visualization of the effect of replacing Cl^- by Br^-. However, these results, together with solution studies (see below) clearly show that the identity of the encapsulated guest causes a shift to the thermal SCO of the $(X@[FeL_3]_2)^{3+}$ species with $T_{SCO}(I) < T_{SCO}(Br) < T_{SCO}(Cl)$.

The encapsulated anion establishes hydrogen bonds with the non-coordinated pyrazole groups of L, thus very removed from the metal centres. Therefore, the influence of the guest on the SCO likely occurs indirectly *via* the N–H···N interactions, involving pyrazole groups that are bound to the metals. These interactions decrease in intensity as X^- gets larger (Table 1), which could be due to steric reasons rather than electronic.

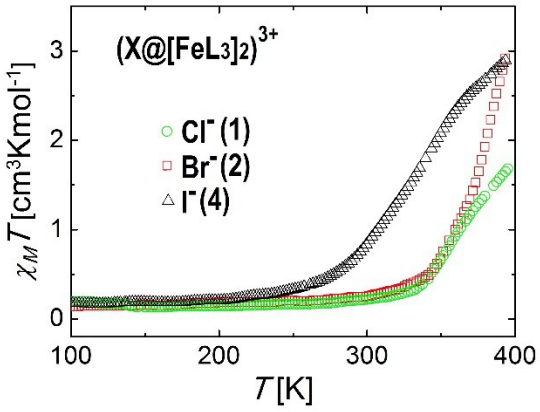

Figure 4. Plots of $\chi_M T$ *vs* *T* for compounds **1**·H_2O, **2**·H_2O and **4**·0.6H_2O·2CH_3OH·2C_3H_6O (measurements were collected on freshly prepared crystals).

The solution stability of the $(X@[FeL_3]_2)^{3+}$ assembly of monomers was investigated by mass spectrometry (MS) and ^1H NMR in acetonitrile. Compound **1** features a set of 16 broad, paramagnetically shifted (6 to 17 ppm) signals, of very similar intensity (Fig. 5). This is in agreement with the shape of the cation, showing only one type of ligand with no symmetry. The group of six signals exhibiting shifts >10 ppm belong to the pyrazolylpyridine moiety bound to Fe(II), which exhibits a very small fraction in the HS state. These shifts are much smaller than for the related dinuclear helicates $(X@[Fe_2L_3])^{3+}$ (up to 62 ppm), consistent with their relative HS/LS populations.[23] The remaining peaks lay within the 6.5 to 7.6 ppm range, not affected by the magnetic moment of HS Fe(II). The N–H resonances are assigned by virtue of their enhanced broadness, the protons being engaged in hydrogen bonds and exchangeable. A number of very minor peaks are also present up to 75 ppm (not shown). The large shifts indicate that some of these could be attributed to the dinuclear $[Fe_2L_3]^{4+}$ species (with and without encapsulated Cl^-, see below). In addition, the presence of Cl-free assemblies of the type $[FeL_3]_2^{4+}$ is noted. The identity of all these minor species is confirmed by MS which, in addition to the major component, reveals their presence (Figs. S8 and S9). These experiments confirm the stability of $(Cl@[FeL_3]_2)^{3+}$ in acetonitrile and the formation of the other possible assemblies in much smaller proportion, as was also demonstrated for the dinuclear helicates $(X@[Fe_2L_3])^{3+}$.[23]

The ^1H NMR of compound **2** (Fig. S10) is similar to that of **1**, confirming the stability in solution of the cation made of monomers $(Br@[FeL_3]_2)^{3+}$, and the marginal formation of the other supramolecular entities. The overall paramagnetic shifts are only slightly larger, in agreement with a similar though larger fraction of HS Fe(II) centres. MS experiments reveal the presence of the Br-free dimer of monomers $([FeL_3]_2)^{4+}$ and dimetallic assembly $([Fe_2L_3])^{4+}$ (Fig. S11), while, as seen for the corresponding dinuclear $(Br@[Fe_2L_3])^{3+}$ helicates,[19] no species incorporating the Br^- guest were detected. This is ascribed to difficulties for these fragments to reach the set up detector. The spectrum of **3** features two sets of 16 signals with similar intensity, and different degrees of paramagnetic shift (Fig. S12). As shown by solid state magnetic measurements, the assembly of monomers $(I@[FeL_3]_2)^{3+}$ exhibits around 25% of Fe in the HS state, thus, suffering a larger paramagnetic shift. The less shifted set corresponds to the dimer $([FeL_3]_2)^{4+}$. The size of I^- prevents the formation of the hypothetical dimetallic cation $(I@[Fe_2L_3])^{3+}$. In this case, no supramolecular species are observed in the MS. The nearly 50:50 proportion between dimers of monometallic complexes $(I@[FeL_3]_2)^{3+}$ and $([FeL_3]_2)^{4+}$, reflects a larger degree of conversion of the former into the latter, perhaps driven by the oxidation of I^- into I_3^-.

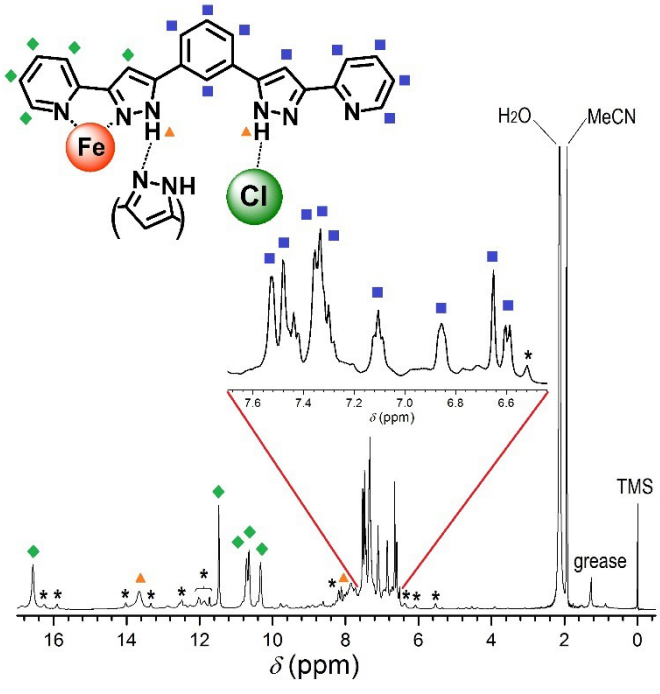

Figure 5. ^{1}H NMR spectrum of **1** in d_3-MeCN at room temperature, evidencing the stability of the $(Cl@[FeL_3]_2)^{3+}$ species in solution. The asterisks correspond very minor supramolecular species (see text).

In conclusion, the properly disposed functional groups of L facilitate its coordination to Fe(II) providing a good environment for the SCO and also, drive the formation of the cationic supramolecular assembly $(X@[FeL_3]_2)^{3+}$ *via* hydrogen bonds and π···π interactions. This species has the flexibility to encapsulate anions with very different sizes (Cl^-, Br^-, I^-) thereby enabling the modulation of its SCO temperature, which is seen to decrease with increasing the size of the guest, as seen in the solid state and also in solution. This underscores once again the potential of supramolecular chemistry to access and manipulate molecular objects with functional properties. This concept will be applied for the encapsulation of other species with optical or magnetic functions, such as coordination complexes.

GA thanks the Generalitat de Catalunya for the prize *ICREA Academia 2008* and *2013* and the ERC for a Starting Grant (258060 FuncMolQIP). The authors thank the Spanish MICINN for funding through CTQ2012-32247, CTQ2015-68370-P (GA, LAB, MD) and MAT2014-53961-R (OR). MD thanks Avempace II Erasmus Mundus Action 2 program for a PhD scholarship. The Advanced Light Source is supported by the Director, Office of Science, Office of Basic Energy Sciences of the U. S. Department of Energy under contract no. DE-AC02-05CH11231.

1. J.-M. Lehn, *Supramolecular Chemistry*, Wiley-VCH Verlag GmbH & Co. KGaA, 2006.
2. J. W. Steed and J. L. Atwood, *Supramolecular Chemistry, 2nd Edition*, John Wiley & Sons, Inc., 2009.
3. D. W. Johnson and F. Hof, *Aromatic Interactions : Frontiers in Knowledge and Application*, The Royal Society of Chemistry, 2017.
4. B. J. Holliday and C. A. Mirkin, *Angew. Chem., Int. Ed.*, 2001, **40**, 2022-2043.
5. G. F. Swiegers and T. J. Malefetse, *Chem. Rev.*, 2000, **100**, 3483-3537.
6. V. Balzani, A. Credi, F. M. Raymo and J. F. Stoddart, *Angew. Chem., Int. Ed.*, 2000, **39**, 3349-3391.
7. V. Balzani, M. Gomez-Lopez and J. F. Stoddart, *Acc. Chem. Res.*, 1998, **31**, 405-414.
8. L. Fabbrizzi and A. Poggi, *Chem. Soc. Rev.*, 1995, **24**, 197-202.
9. O. Kahn, *Acc. Chem. Res.*, 2000, **33**, 647-657.
10. U. Knof and A. von Zelewsky, *Angew. Chem., Int. Ed.*, 1999, **38**, 302-322.
11. I. Beletskaya, V. S. Tyurin, A. Y. Tsivadze, R. Guilard and C. Stern, *Chem. Rev.*, 2009, **109**, 1659-1713.
12. R. A. Bilbeisi, S. Zarra, H. L. C. Feltham, G. N. L. Jameson, J. K. Clegg, S. Brooker and J. R. Nitschke, *Chem., Eur. J.*, 2013, **19**, 8058-8062.
13. Y. Bodenthin, G. Schwarz, Z. Tomkowicz, M. Lommel, T. Geue, W. Haase, H. Moehwald, U. Pietsch and D. G. Kurth, *Coord. Chem. Rev.*, 2009, **253**, 2414-2422.
14. E. Breuning, M. Ruben, J. M. Lehn, F. Renz, Y. Garcia, V. Ksenofontov, P. Gutlich, E. Wegelius and K. Rissanen, *Angew. Chem., Int. Ed.*, 2000, **39**, 2504-2507.
15. F. Tuna, M. R. Lees, G. J. Clarkson and M. J. Hannon, *Chem., Eur. J.*, 2004, **10**, 5737-5750.
16. N. Struch, J. G. Brandenburg, G. Schnakenburg, N. Wagner, J. Beck, S. Grimme and A. Luetzen, *Eur. J. Inorg. Chem.*, 2015, 5503-5510.
17. T. Matsumoto, G. N. Newton, T. Shiga, S. Hayami, Y. Matsui, H. Okamoto, R. Kumai, Y. Murakami and H. Oshio, *Nature Commun.*, 2014, **5**, 3865.
18. B. A. Leita, B. Moubaraki, K. S. Murray and J. P. Smith, *Polyhedron*, 2005, **24**, 2165-2172.
19. M. Steinert, B. Schneider, S. Dechert, S. Demeshko and F. Meyer, *Inorg. Chem.*, 2016, **55**, 2363-2373.
20. M. B. Duriska, S. M. Neville, B. Moubaraki, J. D. Cashion, G. J. Halder, K. W. Chapman, C. Balde, J. F. Létard, K. S. Murray, C. J. Kepert and S. R. Batten, *Angew. Chem., Int. Ed.*, 2009, **48**, 2549-2552.
21. T. Shiga, E. Oshiro, N. Nakayama, K. Mitsumoto, G. N. Newton, H. Nishikawa and H. Oshio, *Eur. J. Inorg. Chem.*, 2013, **2013**, 781-787.
22. C. J. Schneider, B. Moubaraki, J. D. Cashion, D. R. Turner, B. A. Leita, S. R. Batten and K. S. Murray, *Dalton Trans.*, 2011, **40**, 6939-6951.
23. M. Darawsheh, L. A. Barrios, O. Roubeau, S. J. Teat and G. Aromí, *Chem., Eur. J.*, 2016, **22**, 8635-8645.
24. N. Guex and M. C. Peitsch, *Electrophoresis*, 1997, **18**, 2714-2723.
25. P. Pyykkö and M. Atsumi, *Chem., Eur. J.*, 2009, **15**, 186-197.
26. L. S. Harimanow, K. H. Sugiyarto, D. C. Craig, M. L. Scudder and H. A. Goodwin, *Aust. J. Chem.*, 1999, **52**, 109-122.
27. G. Aromi, C. M. Beavers, J. S. Costa, G. A. Craig, G. M. Espallargas, A. Orera and O. Roubeau, *Chem. Sci.*, 2016, **7**, 2907-2915.